

LOAD BEARING BEHAVIOUR IN STRUCTURES DURING PARTIAL  
UPLIFT OF THE BASE MAT DUE TO EARTHQUAKES

H. Wölfel (I)  
W. Breuer (II)  
M. Schalk (III)

Presenting Author: H. Wölfel

SUMMARY

For structures in regions with strong seismic activity it is of main importance to guarantee the global and local stability. The calculated area of separation between base mat and soil depends largely on the solution procedure that is used to investigate the global overturning safety. The same is true with the size of the vertical loads (dead load and inertia loads) that have to be transmitted from the lifted part of the structure (longitudinal wall) to the supported part on the soil by the lateral walls. In the presented paper the differences between the conventional quasistatic analysis and a more realistic dynamic analysis of the turnover of a structure are shown.

INTRODUCTION

In static design the global stability (turnover, frictional resistance, soil pressure) and local stability (integrity and load bearing capacity of structural parts) must be guaranteed. Buildings in regions of stronger seismic activity may partially uplift for a short time. This is mainly true for long, boxlike buildings of nuclear power plants during lateral excitation for the load case safe shutdown earthquake (SSE). If the building is stiffened by outer walls only (Fig. 1), the additional vertical forces that must be transmitted by these walls during uplift may be of the same size like the horizontal forces. Furthermore the uplifted longitudinal wall must transmit the total loads of the building to the lateral walls without direct support. In the past the inherent cross-sectional forces - starting from the results of a linear, dynamic analysis - have been calculated by simple, quasistatic analysis. This method resulted in a considerable amount of additional reinforcement.

In the following the possible procedures to calculate the global and local stability are described and the results compared. For clarity only horizontal excitation is considered. The earthquake excitation is described by a time history, matched to the USNRC-spectrum. The amplitude of acceleration is chosen so that an uplift of the building is evident.

- (I) President of Wölfel Consulting Engineers, D-8706 Höchberg, FRG
- (II) Manager of Structural Mechanics Division of Wölfel Consulting Engineers
- (III) Vice President of Wölfel Consulting Engineers

## CONVENTIONAL ANALYSIS

### Global Safety Against Turnover

The maximum edge pressure and the area of separation may be calculated in a simple way by the assumption of constant soil stiffness and a rigid base mat (Fig. 2). The maximum base moment, that operates due to linear dynamic analysis for only a short time, is taken as effective static turnover moment. The stability is guaranteed, if  $\sigma_{\text{edge}} < \sigma_{\text{max}}$  and  $l_{\text{contact}} > l/2$ . If  $l_{\text{contact}} < l/2$ , a more realistic assumption for the distribution of soil stiffness is necessary. If  $\sigma_{\text{edge}} > \sigma_{\text{max}}$  a realistic analysis of soil failure is necessary.

As a more realistic model (for stiff buildings) the soil stiffness may be distributed in accordance with the theory of a rigid base on an homogeneous, elastic half space. This theory states that the rocking stiffness  $k_{\phi}$ , referred to the longitudinal axis of a rectangular base mat, is about three times larger than  $k_{\phi}$  by the assumption of a constant distribution of the resulting vertical soil stiffness  $k_z$ . This is in accordance with the concentration of the vertical springs at the edges of the base mat. In Fig. 3 the large influence of the assumed distribution of the soil springs on the resulting amount of uplift is shown. For the most favourable case it may be shown that the base mat and soil don't separate even by static analysis if  $M_{\text{max}} < M_{\text{limit}} = (G \cdot l)/2$ . If  $M_{\text{max}} > M_{\text{limit}}$ , it will be only possible by nonlinear dynamic analysis to demonstrate the safety against turnover.

### Local Stability

The state of art is the design of the joint between the longitudinal and lateral walls for the supporting forces that are active during the time of uplift. The equality between soil pressure and dead load is usually not taken into account for the longitudinal walls. These forces are only considered in the design of the base slab. The maximum lateral forces in the uplifted longitudinal wall are calculated by superposition of the inertia forces - calculated with the maximum vertical acceleration at the edge of the building - as additional loads to the dead load (Fig. 4). This is a rather conservative calculation because the inertia forces may be directed opposite to the dead load and the maximum vertical acceleration may not coincide with the time of uplift.

## REALISTIC ANALYSIS

An analysis with consideration of gapping between base mat and soil, i.e. nonlinear dynamic analysis, will be necessary, if the mentioned quasistatic analysis don't result in acceptable design criteria. Because the scope of this paper is not the analysis of a real building with given excitation, a simple plane model is chosen to idealize the vibration in lateral direction. This model is sufficient to demonstrate the phenomenons of vibration with separation of base mat and soil.

### Method of Analysis

Vibration model: The vibration model (Fig. 5) represents the stiffness of the lateral walls and assumes the longitudinal walls to be rigid. Dimensions, masses and stiffnesses are matched to a real nuclear power plant building. The soil is modelled by springs and dashpots. The global stiffnesses  $k_y$  and  $k_z$  of

the springs are determined by use of the theory of elastic half space and are distributed according to the influence area of the nodal points ( $k_y$  proportional to the area and  $k_z$  proportional to the circumference). Two cases of soil stiffness are examined. In Fig. 6 the controlling natural modes for horizontal vibration are shown together with the most important parameters.

Scope of analysis: The following topics of vibration behaviour are investigated in detail:

- vibration characteristic in general
  - global turnover moment
  - separation of base mat and soil
  - working direction of inertia forces
  - supporting forces of longitudinal wall
- |   |                  |
|---|------------------|
| } | global stability |
| } | local stability  |

To value the influence of partial uplift, two models are investigated. The first that will be called linear (L-) model in the following, is based on the assumption that the vertical springs transmit compression as well as tension. For the second nonlinear (NL-) model only the transmission of pressure forces is possible by the vertical springs.

Calculation method: Time history modal analysis is used for the L-model while the controlling quantities are calculated by direct integration for the NL-model. The coefficients of Rayleigh-damping in the NL-model are matched as well as possible to the modal dampings of the L-model. The vertical springs in the NL-model are assumed to be linear elastic in compression ( $F < 0$ ) and fail in tension ( $F = 0$ ). The frictional, horizontal springs are assumed to be linear elastic in all cases as simplification for the presented investigations.

## Results

Vibration characteristics: The time histories of vertical displacements and accelerations of the corner node no. 1 (Fig. 7 and 8) show only for case 2 (stiff soil) an evident difference in shape and amplitude between L- und NL-model. The NL-model results in considerable larger accelerations, however only during a short time interval.

It is obvious to see from the displacement of the building during first uplift (Fig. 9), that in the NL-model the building is forced to global, vertical vibrations, caused by the shift of the center of active spring stiffness during the loss of one spring.

Global stability: In Fig. 10 and 11 the course of global turnover moment and inherent contact area during the phase of uplift are shown. The moments are compared to the maximum possible turnover moments by conventional quasi-static analysis (compare Fig. 3).

The NL-model results in a turnover moment that may be larger than the maximum static turnover moment because the produced inertia forces without failure of global stability, i.e. the safety against turnover is guaranteed despite a safety factor  $\nu < 1$ . The largest amount of uplift and the maximum moment appear at different times in consequence of the global, vertical inertia forces that contribute widely to the turnover moments.

Local stability: It is shown in Fig. 12 for case 1 that vertical displacement and acceleration are usually in opposite direction, i.e. the inertia forces of the longitudinal wall are opposed to the dead loads at the uplifted side. A more closely look at the beginning of uplift (Fig. 13), however, shows

that the acceleration may also be positive for a short time interval (40 ms) so that the inertia forces act in addition to the dead load.

If a more general, 3D-model is used, the supporting forces of the longitudinal wall at the side of uplift as well as contact can be computed automatically by the vibration model for the mutual action of inertia forces (+ dead load) and soil pressure. For the used global model the supporting forces have to be calculated by use of equality conditions for inertia forces (+ dead load) and spring forces. In Fig. 14 and 15 the resulting supporting forces in the uplifted wall will be compared with the lateral forces of the longitudinal wall, if the maximum acceleration is used for their calculation instead the actual accelerations during uplift.

#### CONCLUSION

The investigations indicate that a realistic estimation of the safety against turnover during seismic excitation is first of all influenced by realistic assumptions for the distribution of vertical soil stiffness. If it is not possible to guarantee the safety against turnover by quasistatic analysis it may be possible to show the global stability by a nonlinear dynamic analysis even for stronger excitations. The conventional quasistatic analysis results in considerable overestimations of the danger of turnover.

It is proposed to calculate the supporting forces of the uplifted, longitudinal wall either directly in the vibration model, or, by use of a global model, with the actual accelerations during uplift. The use of maximum accelerations results in unrealistic high supporting forces.

#### REFERENCES

- (1) R. Zinn, F. Stangenberg, "Base Mat Uplift Effects on the Seismic Response of a Rectangular Nuclear Building, Paper K9/3 of SMIRT Conference, Chicago 1983
- (2) R.P. Kennedy, S.A. Short, D.A. Wesley, T.H. Lee, "Effect on Non-Linear Soil-Structure Interaction Due to Base Slab Uplift on the Seismic Response of a High-Temperature Gas-Cooled Reactor (HTGR)", Nuclear Engineering and Design 38, 1976, North Holland Publishing Company
- (3) J.P. Wolf, "Approximate Soil-Structure Interaction with Separation of Base Mat from Soil (Lifting-Off)", Nuclear Engineering and Design 38, 1976, North Holland Publishing Company

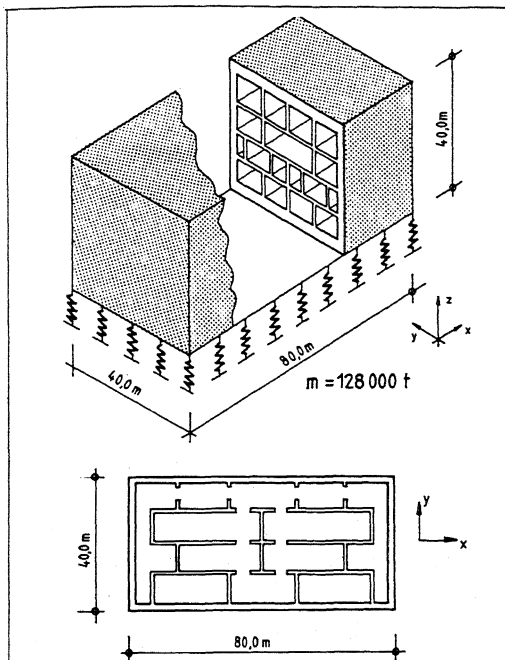


Fig. 1: Type of Structure

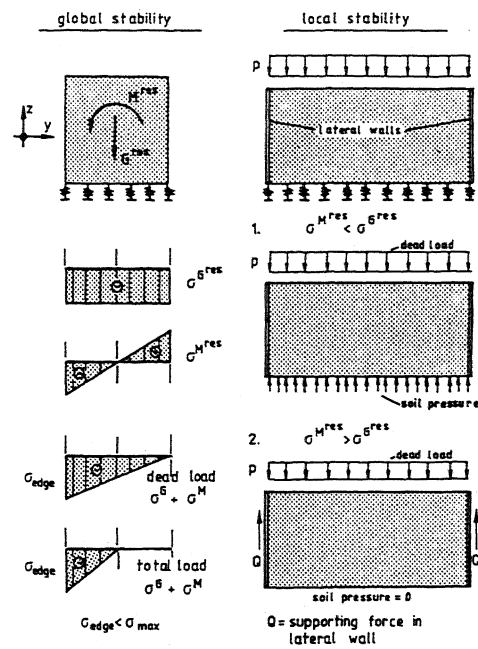


Fig. 2: Stability by Conventional Static Analysis

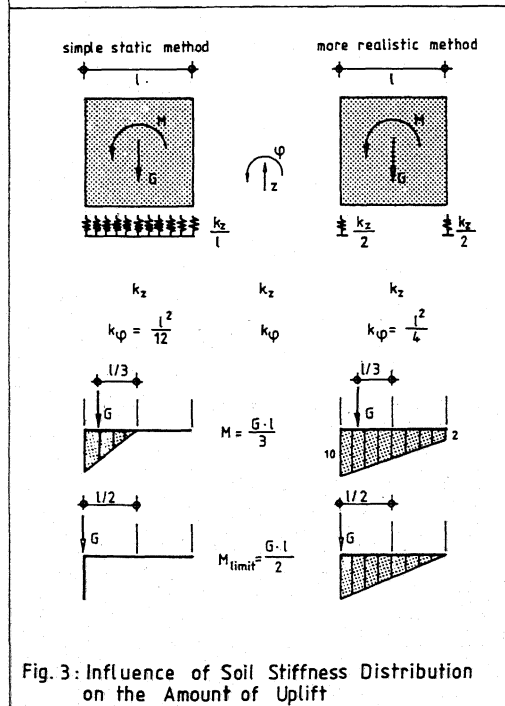


Fig. 3: Influence of Soil Stiffness Distribution on the Amount of Uplift

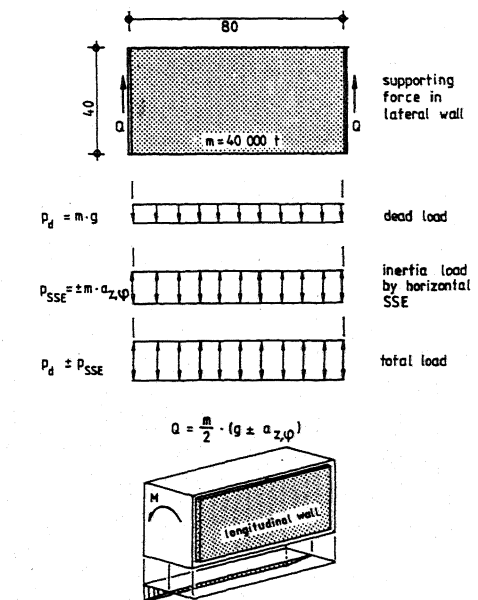


Fig. 4: Local Stability of Longitudinal Wall during Uplift

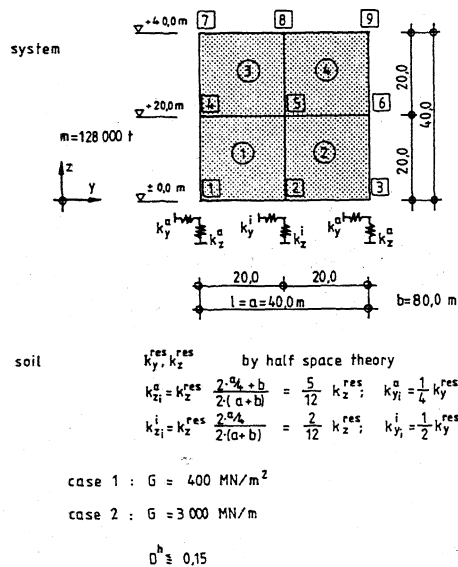


Fig.5: Vibration Model

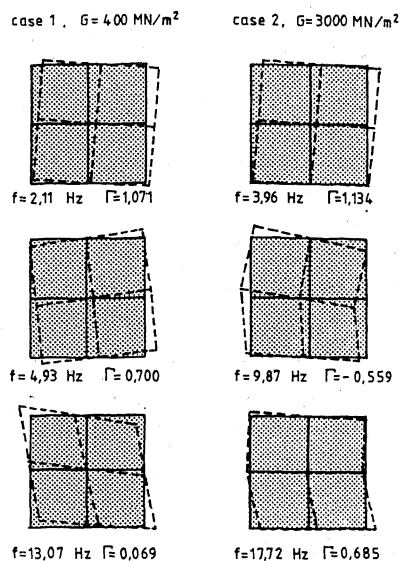


Fig.6: Controlling Natural Modes for Horizontal Excitation

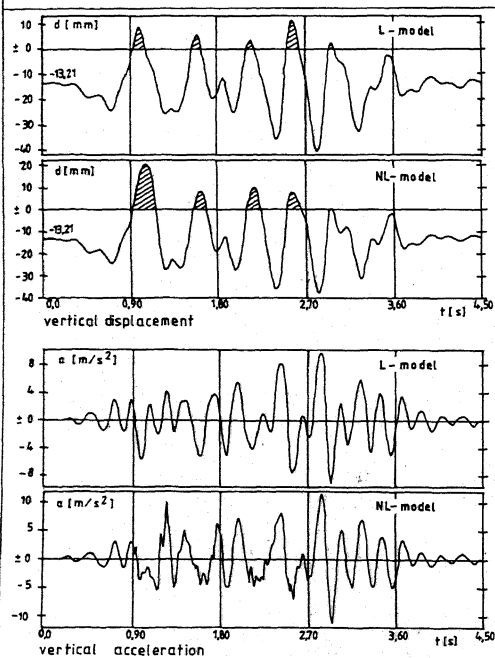


Fig.7: Vertical Response of Corner Node 1  
(Case 1,  $G = 400 \text{ MN/m}^2$ ,  $a_0^h = 10 \text{ m/s}^2$ )

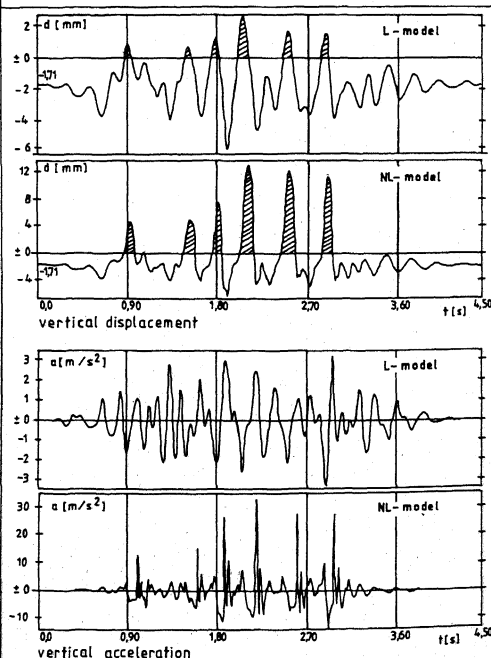


Fig.8: Vertical Response of Corner Node 1  
(Case 2,  $G = 3000 \text{ MN/m}^2$ ,  $a_0^h = 10 \text{ m/s}^2$ )

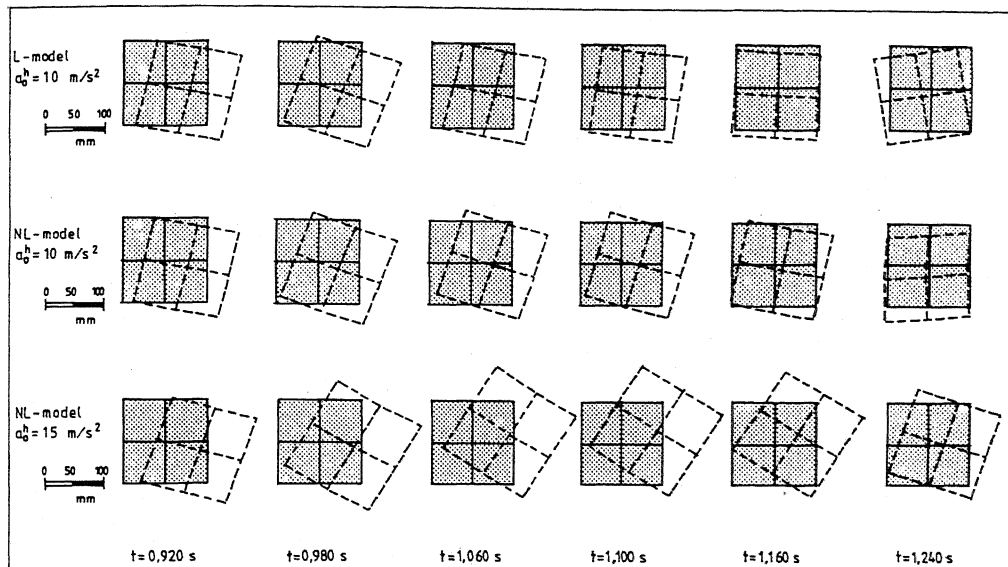


Fig.9: Displacements during First Uplift  
(Case 1,  $G = 400 \text{ MN/m}^2$ )

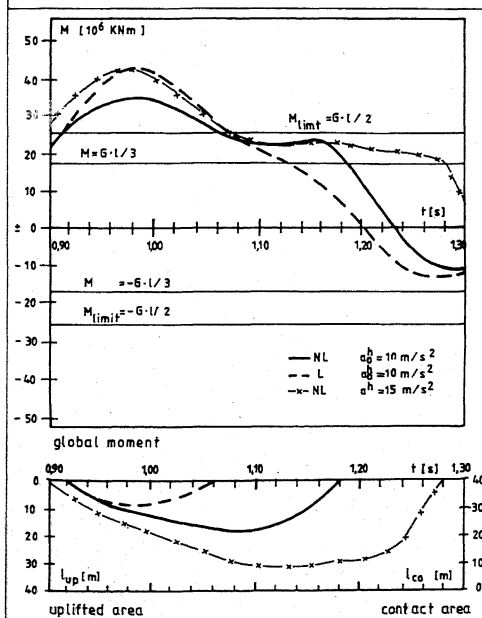


Fig.10: Global Results during Uplift  
(Case 1,  $G = 400 \text{ MN/m}^2$ )

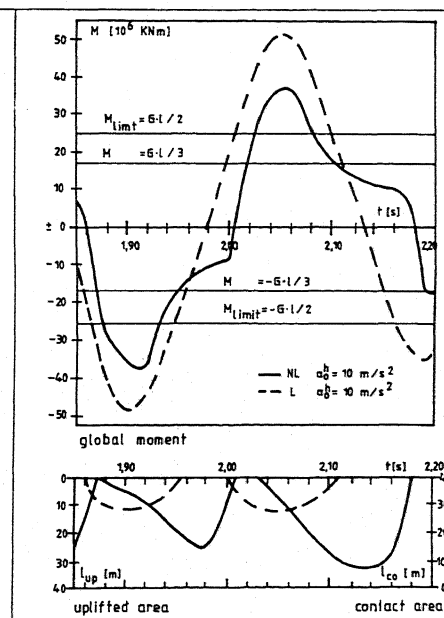


Fig.11: Global Results during Uplift  
(Case 2,  $G = 3000 \text{ MN/m}^2$ )

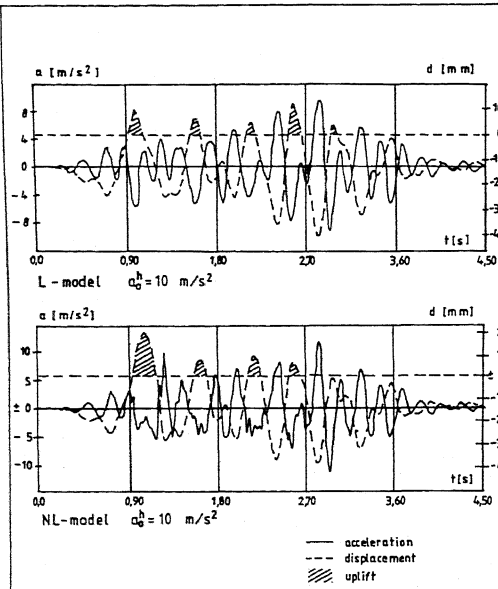


Fig.12: Comparison of the Time Histories of Vertical Displacement and Acceleration (Corner Node 1, Case 1,  $G = 400 \text{ MN/m}^2$ ,  $a_0 = 10 \text{ m/s}^2$ )

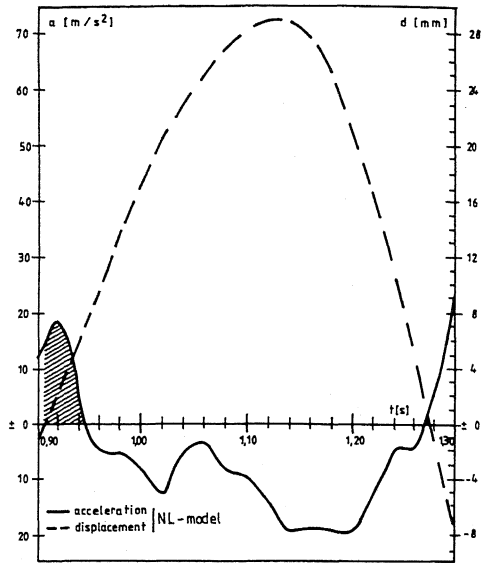


Fig.13: Comparison of the Time Histories of Vertical Displacement and Acceleration during First Uplift (Corner Node 1, Case 1,  $G = 400 \text{ MN/m}^2$ ,  $a_0 = 15 \text{ m/s}^2$ )

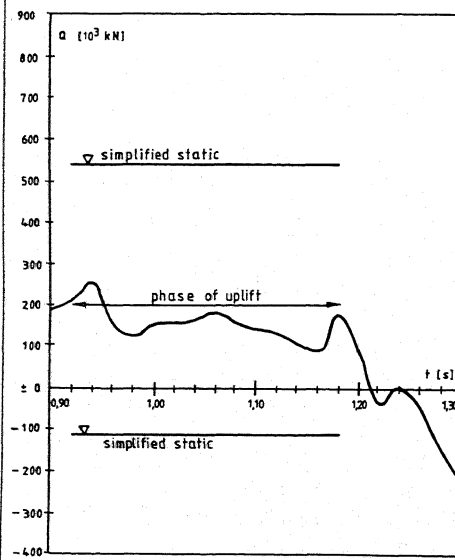


Fig.14: Time History of Supporting Forces of Longitudinal Wall during Uplift (Case 1,  $G = 400 \text{ MN/m}^2$ ,  $a_0 = 10 \text{ m/s}^2$ , NL-Model)

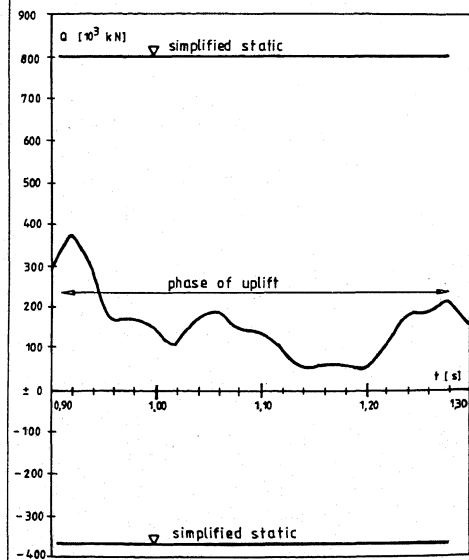


Fig.15: Time History of Supporting Forces of Longitudinal Wall during Uplift (Case 1,  $G = 400 \text{ MN/m}^2$ ,  $a_0 = 15 \text{ m/s}^2$ , NL-Model)